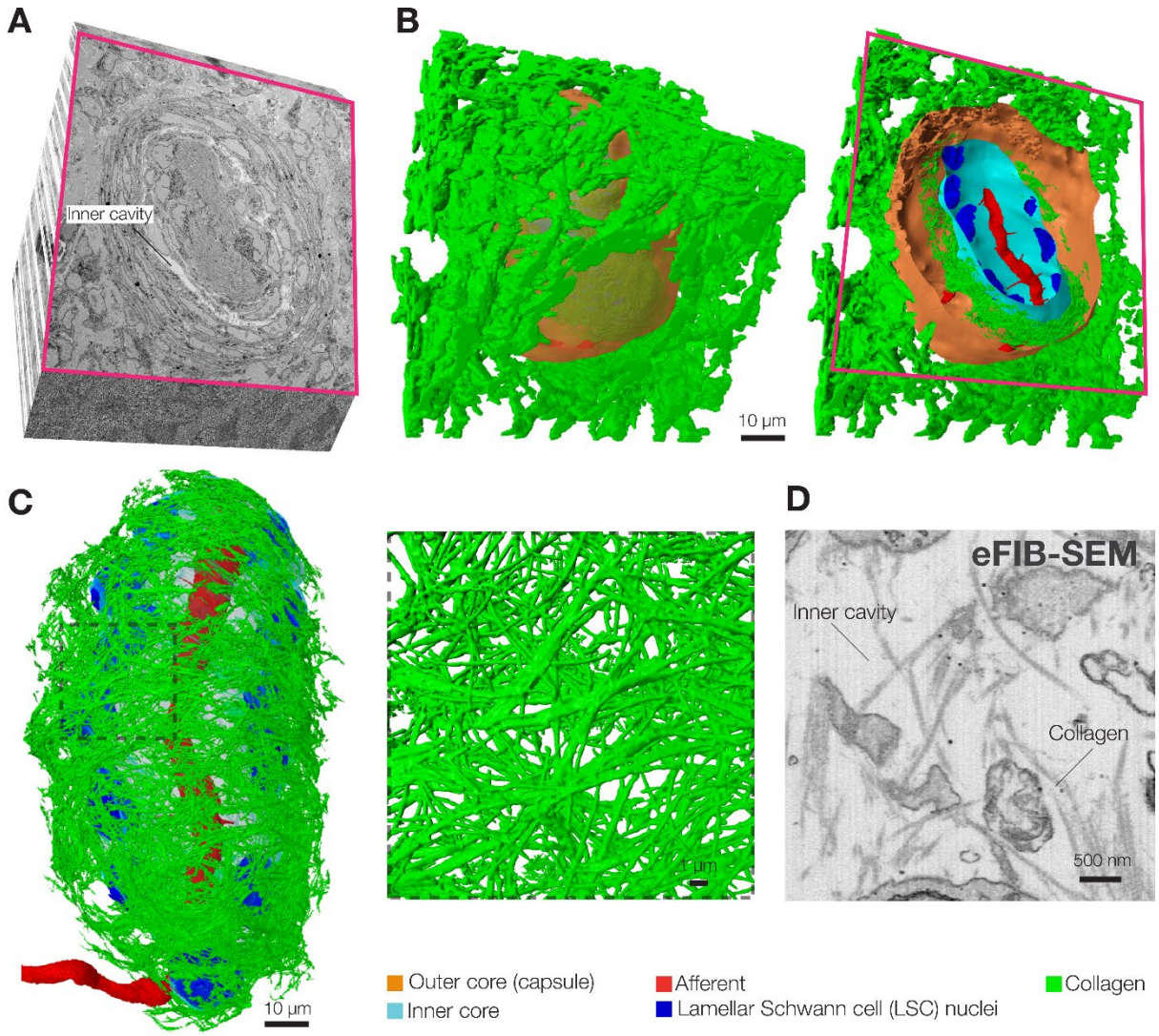

Figure S1. The cavity between the outer and inner cores is filled with collagen fibers.

(A) A cross-section of the 3D volume from eFIB-SEM data showing the location of the inner cavity in the Pacinian corpuscle.

(B) 3D reconstruction of the same volume and a cross-section, as in (A), showing thick collagen bundles surrounding the outer core.

(C) A 3D reconstruction of a Pacinian inner core surrounded by single collagen fibers, along with a magnified region.

(D) eFIB-SEM single image from the inner cavity showing single collagen fibers inside the corpuscle.

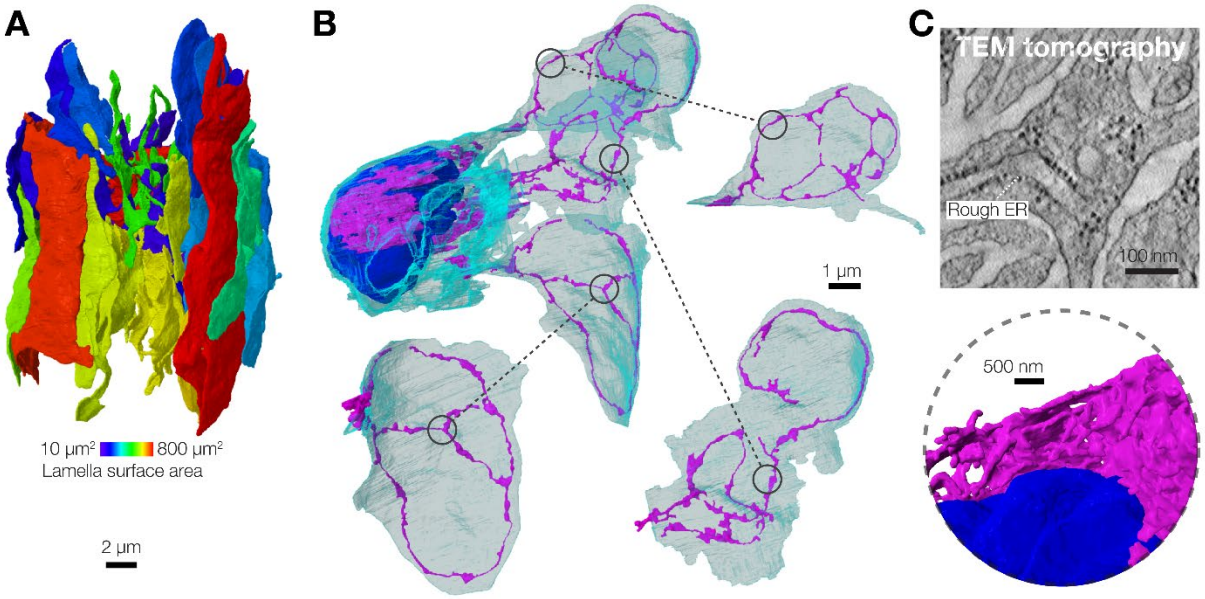

779 **Figure S2. 3D reconstruction of a lamellar Schwann cell from the Pacinian inner core.**

780 (A) 3D reconstruction of an LSC showing surface area of lamellae.

781 (B, C) 3D reconstruction of endoplasmic reticulum (B) and a single FIB-SEM image of rough endoplasmic
782 reticulum (rough ER) in LSC lamellae (C).

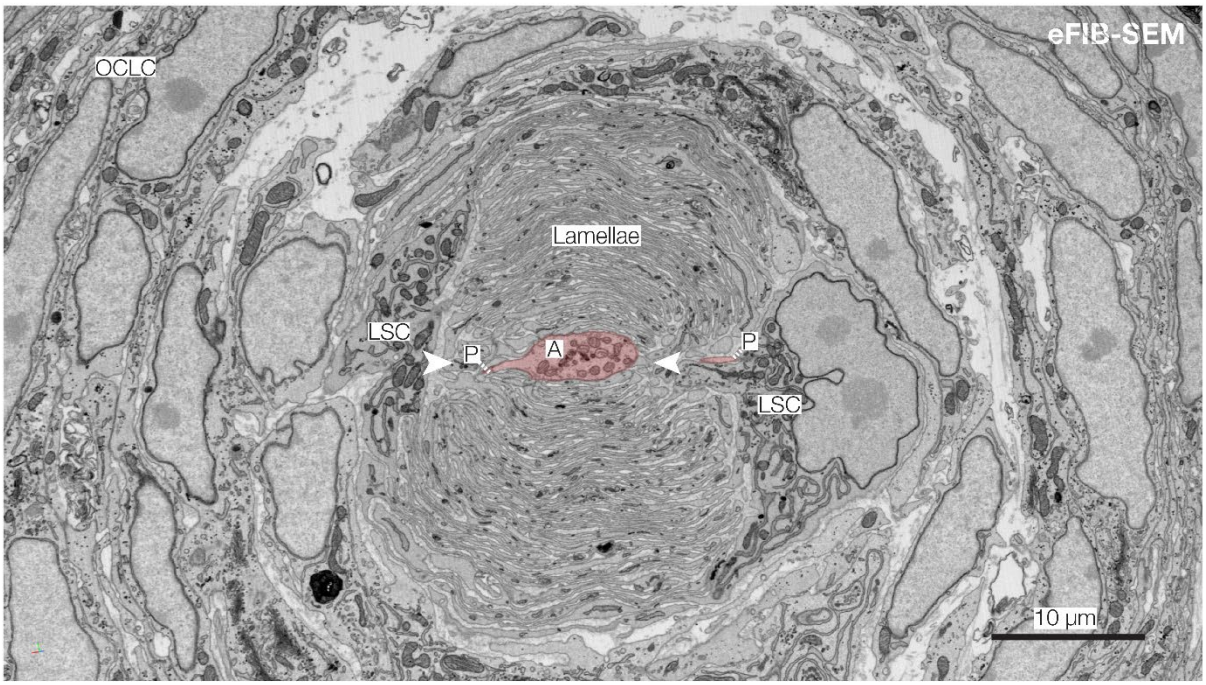

Figure S3. Protrusions emanate from the narrow sides of afferent terminal facing the cleft in LSC lamellae.

Shown is an eFIB-SEM image of a Pacinian inner core. LSC, lamellar Schwann cells, OCLC, outer core lamellar cells, N, LSC nucleus; A, afferent terminal ; P, protrusion. Arrowheadspoint to the cleft formed by inner core lamellae.

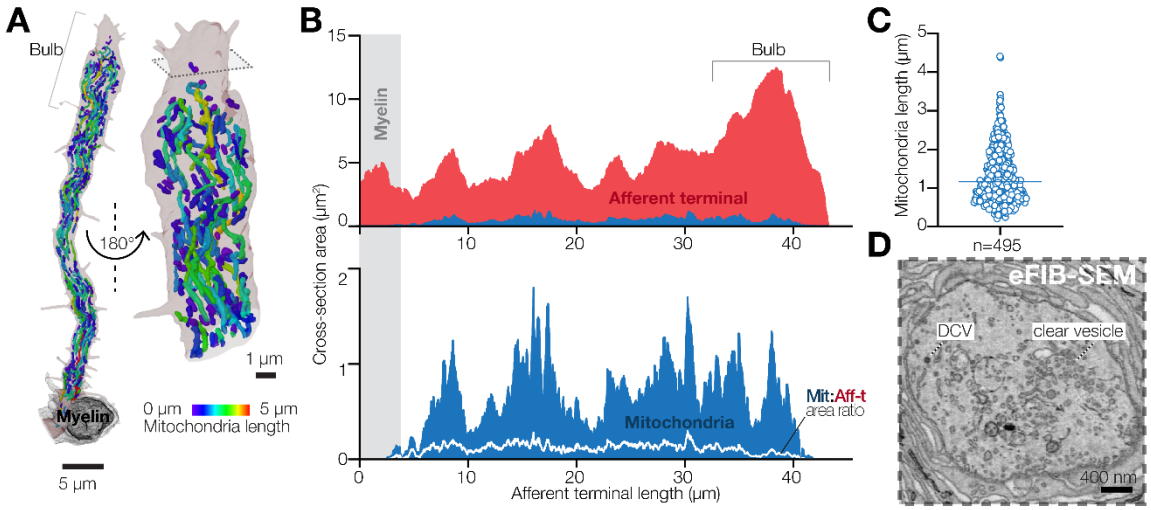

788 **Figure S4. Mitochondria and vesicles in the Pacinian afferent terminal.**

789 (A) 3D reconstruction of mitochondria in the afferent terminal.

790 (B) Quantification of cellular area occupied by mitochondria along the length of the terminal.

791 (C) Quantification of mitochondria length in the afferent terminal.

792 (D) A single eFIB-SEM image of the afferent terminal bulb with clear vesicles and dense core vesicles
793 (DCV).

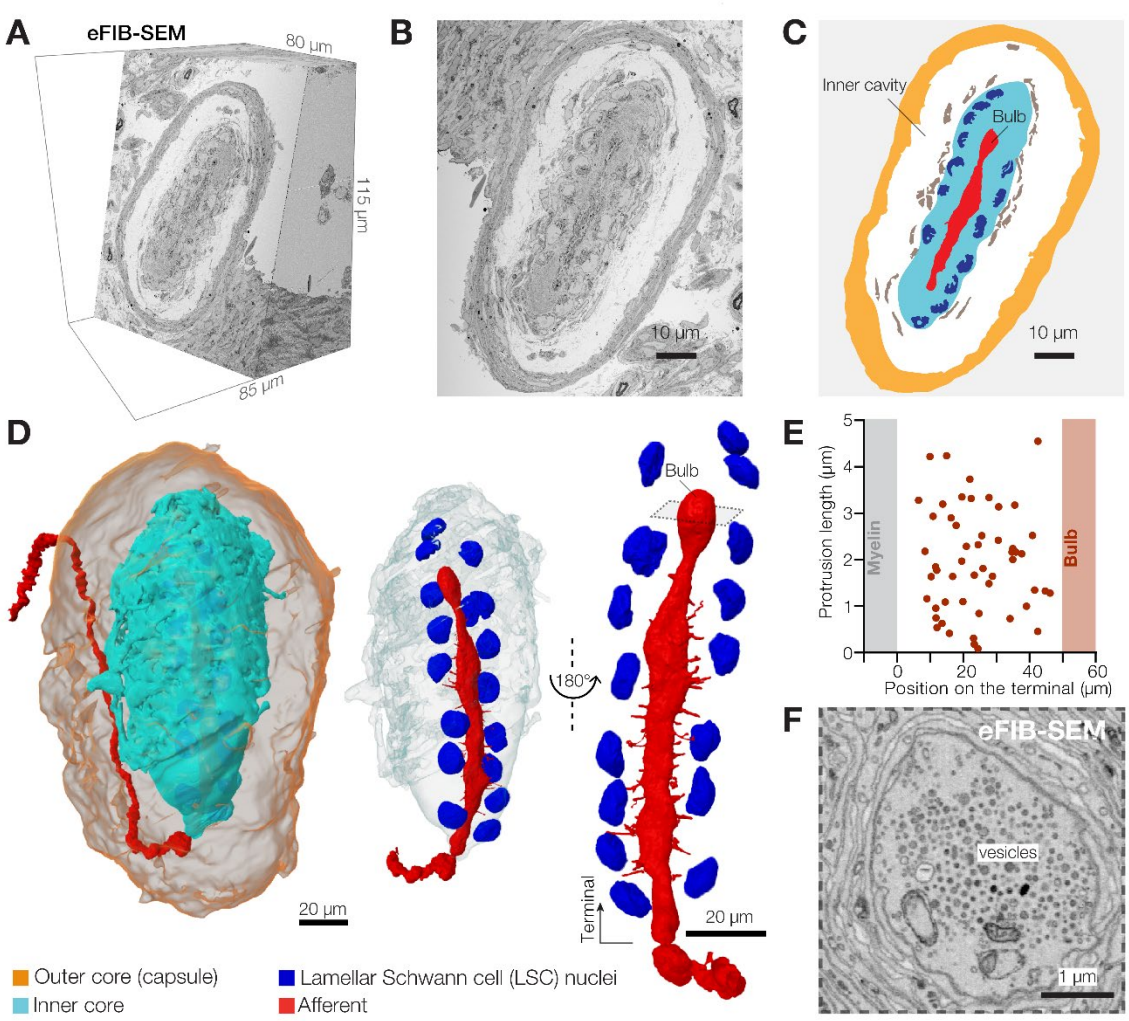

794 **Figure S5. 3D architecture of a second Pacinian corpuscle.**

795 (A) A 3D volume of duck bill skin dermis obtained by eFIB-SEM.

796 (B, C) A single eFIB-SEM image (B) and an illustration (C) of a section of the Pacinian corpuscle.

797 (D) 3D reconstruction of the Pacinian corpuscle showing the location of the inner core inside the outer
798 core, and reconstruction of the inner core and the afferent.

799 (E) Localization, length and target of afferent protrusions in the second Pacinian.

800 (F) A single eFIB-SEM image of the bulb area of the afferent terminal showing clear and dense core
801 vesicles (DCV).

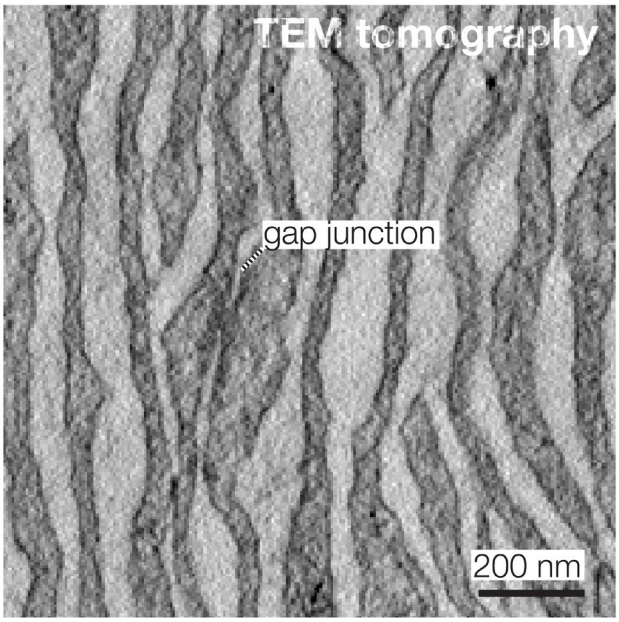

Figure S6. LSC lamellae are connected by gap junctions.

Shown is a transmission electron microscopy image of inner core lamellae connected by a gap junction.

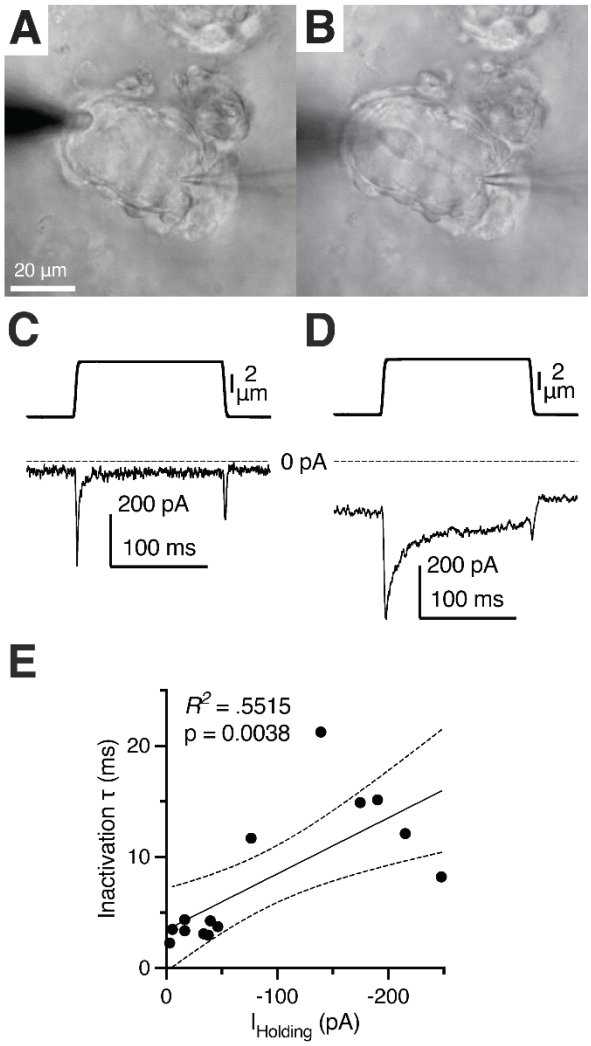

804 **Figure S7. Prolongation of MA current inactivation in a deteriorated Pacinian afferent terminal after**
805 **decapsulation.**

806 (A) Bright-field image of a patched Pacinian terminal in a decapsulated corpuscle.

807 (B) Bright-field image of the deteriorated decapsulated terminal from (A).

808 (C) Mechanical stimulus (top) and MA current response (bottom) of the patched terminal in (A) after
809 decapsulation shows fast kinetics of inactivation.

810 (D) Mechanical stimulus (top) and MA current response (bottom) of the deteriorated decapsulated
811 terminal at the same time point that the image in (B) was captured.

812 (E) Relationship between inactivation rate of MA current in patch-clamped terminals and the holding
813 current applied during voltage clamp at -60 mV, fitted to the linear equation.

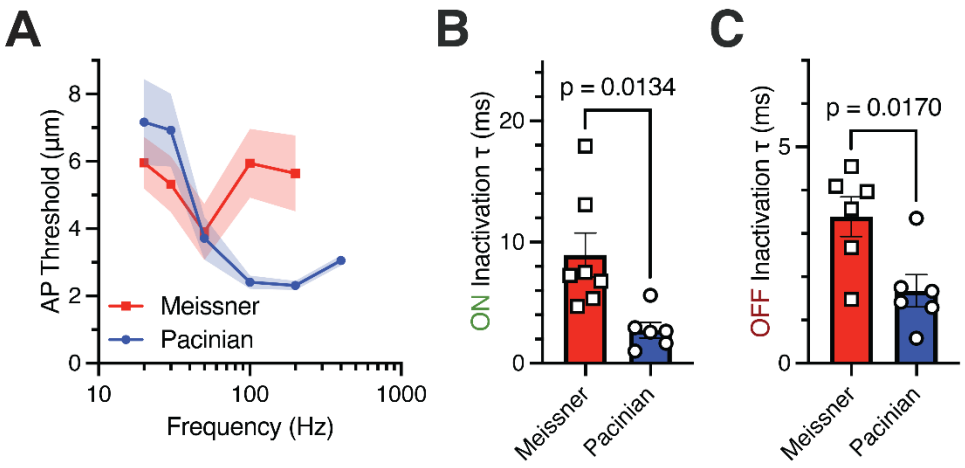

Figure S8. Correlation between peak frequency sensitivity and MA current inactivation in Meissner and Pacinian corpuscles.

(A) Population tuning curves recorded from afferents of avian Meissner and Pacinian corpuscles. Data are shown as mean ± SE from 9 Meissner and 26 Pacinian corpuscles.

(B, C) Rates of MA current inactivation (B, ON response; C, OFF response) recorded from Meissner and Pacinian afferent terminals. Symbols represent recordings from individual corpuscles. Data are shown as mean ± SEM. Statistics: Welch's t-test.

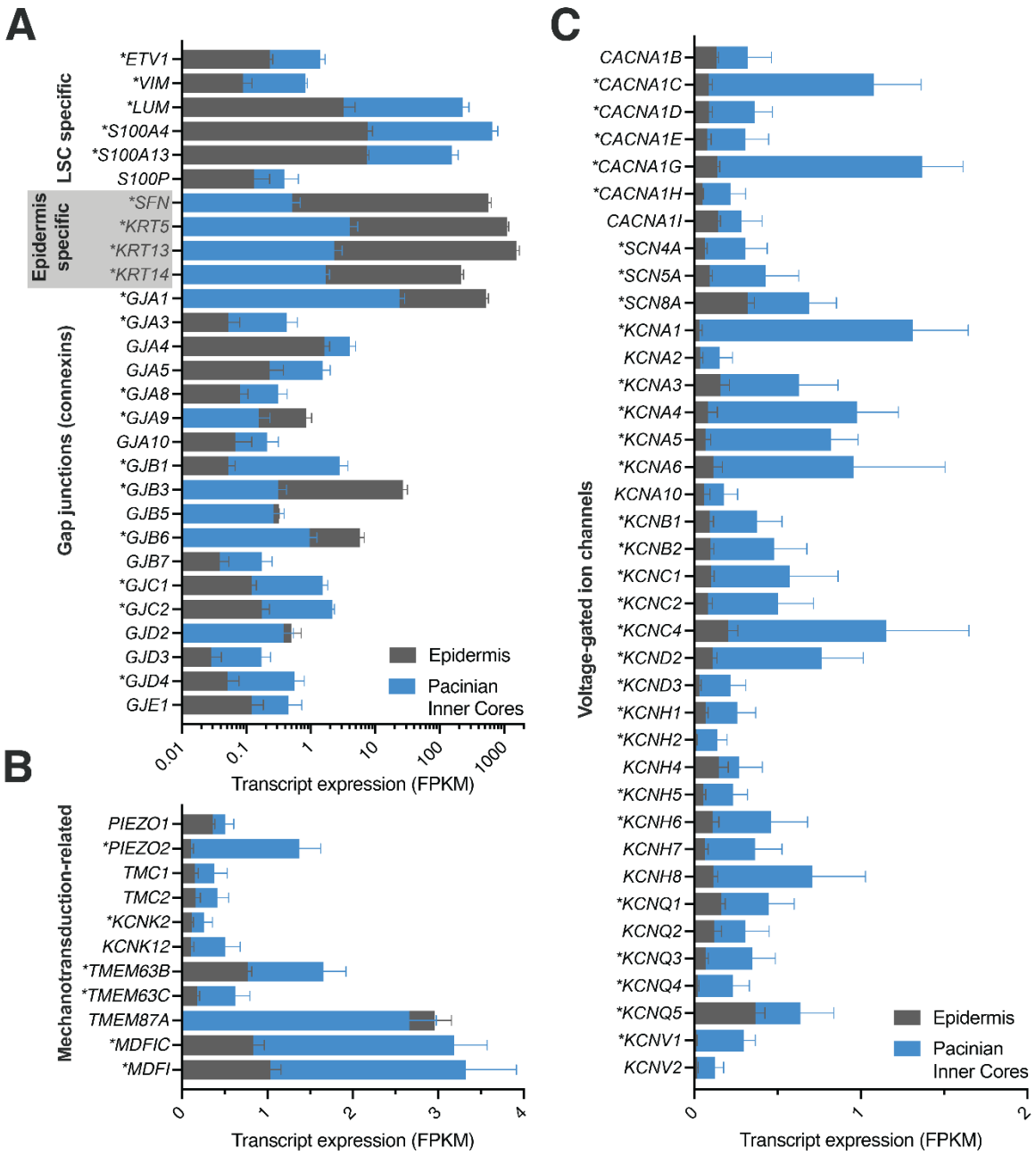

Figure S9. RNA sequencing of Pacinian inner cores.

(A-C) Shown are fragments per kilobase per million reads sequenced from mRNA of genes of (A) gap junction connexins, (B) known and putative mechanically-gated ion channels and their modifiers, (C) voltage-gated sodium, voltage-gated calcium channels, and voltage-gated potassium channels from isolated Pacinian inner cores, compared to expression of such genes in the duck bill epidermis. Data are mean + SEM from 7 inner cores and 6 epidermis samples. Statistics: Fisher's Exact Test with Benjamini-Hochberg method for false discovery rate (FDR) *FDR-adjusted P < 0.05.

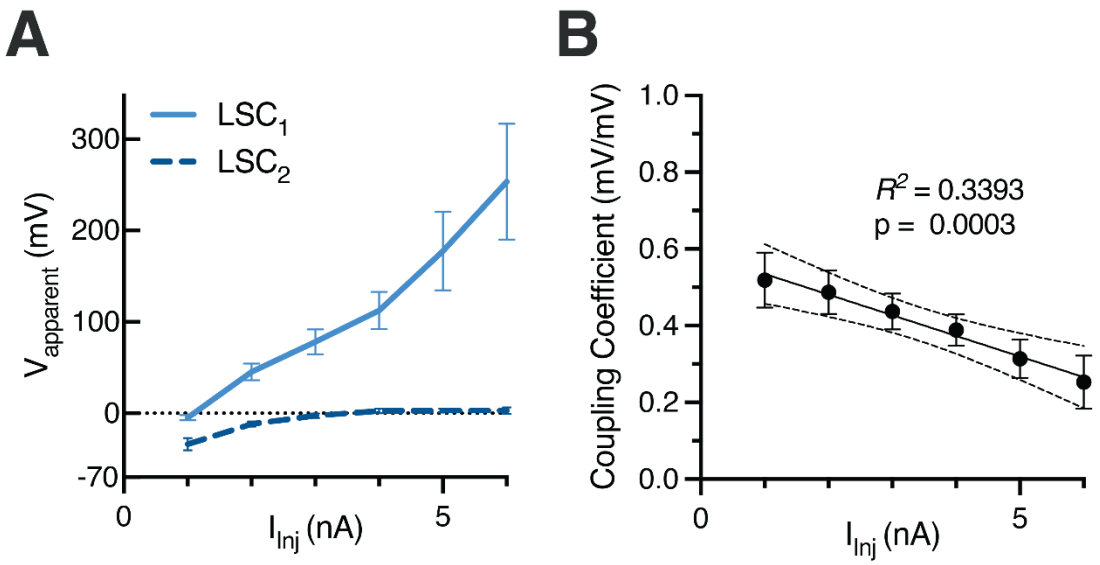

Figure S10. Electrical coupling between adjacent LSCs is voltage-dependent.

(A) Quantification of the effect of current injection into an LSC on the apparent membrane potential of the same and adjacent LSC (LSC_1 and LSC_2, respectively). Data are mean ± SEM from 5 recordings.

(B) The coupling coefficient between LSC pairs from (A). Data are mean ± SEM from 5 recordings, fitted to the linear equation.

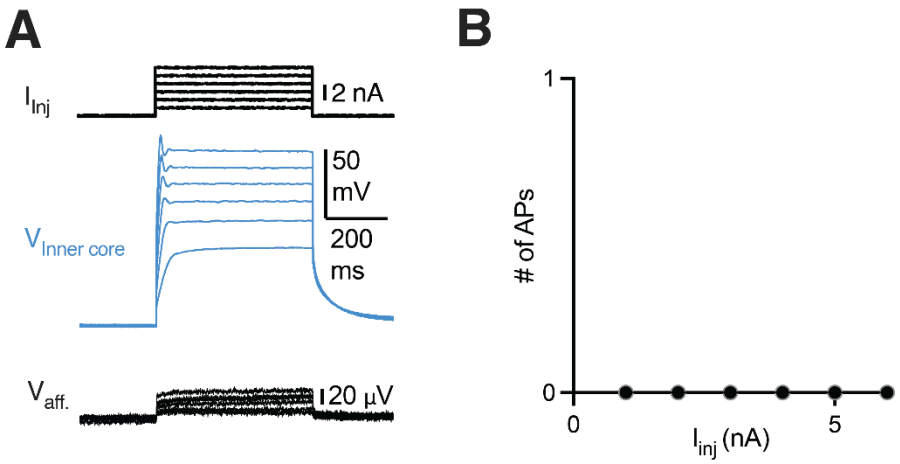

Figure S11. Activation of a single LSC by current injection fails to induce AP firing in the afferent.

(A) Current injection stimulus applied to a patch-clamped LSC (top), voltage response of the patched LSC (middle), and single-fiber response of the associated Pacinian afferent during simultaneous paired recording.

(B) Quantification of the number of action potentials elicited during LSC activation by current injection. Data shown as overlapping lines representing individual cells from 6 recordings (all 0 APs).

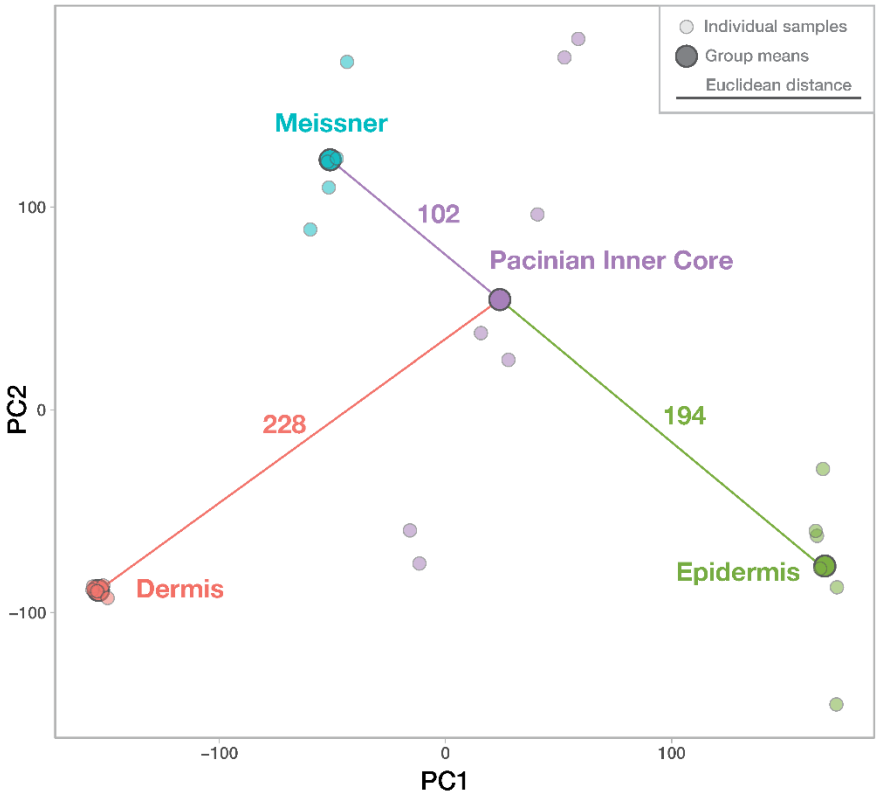

Fig S12. Pacinian inner core is transcriptomically more similar to Meissner corpuscles than to bill skin epidermis or dermis.

A PCA plot (first two principal components) of transcriptomic data from Pacinian inner core and bill skin epidermis (this study), Meissner corpuscles and bill skin dermis (Nikolaev *et al.*, 2023) showing individual samples (small circles) and group means (large circles). Numbers above the connecting lines indicate Euclidean distances between group means. Activation of a single LSC by current injection fails to induce AP firing in the afferent.

846 **Table S1. Accuracy statistics of eFIB-SEM data segmentation for Pacinian corpuscles.**

Method	Object	IoU*	F1 score
eFIB-SEM Pacinian #1	Afferent1	0.67	0.80
	Inner core	0.76	0.86
	Outer core	0.55	0.71
	Collagen	0.65	0.79
	ER (lamellae)	0.75	0.86
	ER (cell body)	0.85	0.92
	Nuclei	0.78	0.88
	Mitochondria	0.58	0.73
	Lamellae	0.75	0.86
eFIB-SEM Pacinian #2	Afferent2	0.85	0.92
TEM tomography Pacinian #1	Afferent	0.98	0.99
	Lamellae	0.95	0.97
	Tethers	0.78	0.88

*Intersection over Union

847 **Movie S1.** 3D architecture of an avian Pacinian corpuscle obtained using eFIB-SEM.

848 **Movie S2.** 3D reconstruction of a fragment of lamellar cell-afferent contact area obtained by transmission
849 electron microscopy tomography.

850 **Supplementary Data S1.** RNA sequencing of Pacinian inner cores vs epidermis. Data were deposited to
851 the Gene Expression Omnibus, accession number GSE273272.